Laser-induced fluorescence studies of excited Sr reactions. III. Sr(P-3(1))+CHF = CH2, CF2 = CH2, CHF = CHF, and C6H5F

Teule, J.M.; Janssen, M.H.M.; Stolte, S.; Bulthuis, J.

published in
Journal of Chemical Physics
2002

DOI (link to publisher)
10.1063/1.1458242

document version
Publisher's PDF, also known as Version of record

Laser-induced fluorescence studies of excited Sr reactions. III. $Sr(^3P_1)+CHF{=}CH_2$, $CF_2{=}CH_2$, $CHF{=}CHF$, and C_6H_5F

J. M. Teule,[a] M. H. M. Janssen, S. Stolte, and J. Bulthuis[b]
Department of Chemistry and Laser Centre, Vrije Universiteit, de Boelelaan 1083, 1081 HV Amsterdam, The Netherlands

(Received 28 November 2001; accepted 17 January 2002)

Laser-induced fluorescence spectra reveal the internal energy distributions of $SrF(X\,^2\Sigma)$ formed in the reactions of electronically excited $Sr(^3P_1)$ with various unsaturated fluorohydrocarbons, i.e., $CHF{=}CH_2$, $CF_2{=}CH_2$, $CHF{=}CHF$, and C_6H_5F. The internal energy distribution of the ground state diatomic product typically shows less vibrational excitation, without inversion, and somewhat lower rotational excitation than the reactions of $Sr(^3P_1)$ with HF and saturated hydrocarbons. The different behavior of the two groups of reactants is rationalized by a simple MO picture, assuming that an electron from Sr is transferred to a σ^* orbital in HF and the saturated fluorohydrocarbons and to a π^* orbital in the unsaturated fluorohydrocarbons with a subsequent transfer to a σ^* orbital of the C–F bond. The latter transfer constitutes an extension of the reaction path, leading to less vibrational excitation. This would explain why the energy disposal in the reaction with C_6H_5F behaves similar to that in the reactions with the fluoroethenes. Even if the shape of the vibrational distribution of the SrF product is the same for all unsaturated fluorohydrocarbons studied, the degree of vibrational excitation varies strongly. This even holds when comparing *cis*- and *trans*-$CHF{=}CHF$, where the distributions can be characterized by distinct surprisal parameters. © *2002 American Institute of Physics.* [DOI: 10.1063/1.1458242]

I. INTRODUCTION

In the pursuit of a better understanding of the reaction mechanism and the distribution of the available energy in reactions of $Sr(^3P_1)$ with fluorine containing molecules,[1–3] in this paper we focus on reactions of $Sr(^3P_1)$ with unsaturated fluorohydrocarbons.

Gas-phase reactions between alkaline earth metals M and halogen containing molecules RX have been studied extensively, but not much is known about the influence of the presence of a double bond in the R group. A number of studies looked into reactions of metal atoms with aromatic halides.[4–6] In this context Han, He, and Lou[4] suggested that the valence electron of the alkaline earth metal is transferred into the π^* orbital of the benzene ring, and subsequently transferred into the σ^* orbital of the C–X bond. In their study of the reaction $Ba+C_6H_5X\rightarrow BaX+C_6H_5$ (X=I, Br, Cl), this hypothesis explains the increase in the amount of energy disposed into BaX vibration in going from C_6H_5I to C_6H_5Cl. Reactions of Ba with CH_3X show an opposite trend in vibrational energy disposal. Both trends are explained with the increase and decrease of the LUMO (lowest unoccupied molecular orbital) energies in going from Cl to I for the reactions with C_6H_5X and CH_3X, respectively.

Brenner, Smith, and Zare[6] observed very low vibrational and rotational excitation of the BaCl products formed in the reactions $Ba+C_6H_5CH_2Cl$, $C_6H_4CH_3Cl$, with the largest part of the reaction energy being disposed as translational energy or internal energy of the organic radical.

In previous papers,[1,2] parts I and II of this series, the product internal energy distributions of reactions between $Sr(^3P_1)$ and HF,[1] CH_3F, C_2H_5F, and $C_2H_4F_2$[2] were presented. Electronic excitation of Sr to the $^3P_1$ state was necessary for all reactions to observe $SrF(X\,^2\Sigma)$ reaction products in our experiments. Large variations in reaction energy disposal were observed by studying the vibrational and rotational energy distributions in the SrF products.

In this study we present the vibrational and rotational population distributions in the $SrF(X\,^2\Sigma)$ products formed in the reactions of $Sr(^3P_1)$ with $CHF{=}CH_2$, $CF_2{=}CH_2$, $CHF{=}CHF$ (*cis*, *trans*), and C_6H_5F. The energetics are shown in Fig. 1. The exoergicity for all reactions is around 2.2 eV, slightly less than for the saturated compounds. The product energy distributions are deduced from the laser-induced fluorescence (LIF) spectra using spectrum simulation.

II. EXPERIMENT

As described in earlier papers on this subject,[1–3] the experiments are done in a beam-gas apparatus, where the Sr atoms effuse out of an oven kept at 900 K. The metal vapor diffuses into a vacuum chamber, where it intersects a 689.3 nm laser beam from a frequency-stabilized linear titanium: sapphire laser (Spectra Physics Model 3900S, 600–1000 nm). The Ti:sapphire laser is pumped by 4 W of an argon ion laser (Spectra Physics Model 2030, 15 W output all lines), yielding about 70 mW laser power in the scattering chamber.

[a]Present address: Art Innovation bv Holland, Westermaatsweg 11, 7556 BW Hengelo, The Netherlands.
[b]Electronic mail: bulthuis@chem.vu.nl

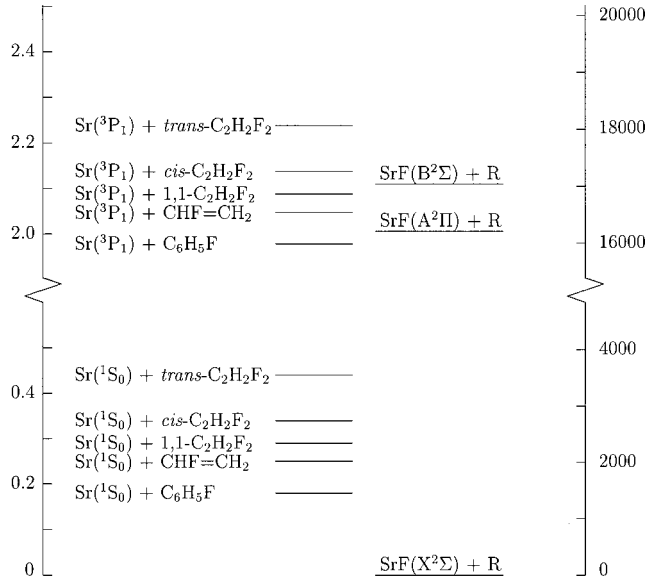

FIG. 1. Energetics for the reactions $Sr(^1S_0, {}^3P_1)+CHF=CH_2$, $C_2H_2F_2$, C_6H_5F, and $C_2H_4F_2$ (energy on the left axis in eV, on the right axis in cm^{-1}).

In this way approximately 2% of the Sr atoms (number density 3×10^{10} cm^{-3}) are electronically excited to the metastable $[5s5p(^3P_1)]$ state.

The reactant gas is admitted into the vacuum chamber through a needle valve until the pressure is 1×10^{-4} Torr. Studying the reaction with 1,2-difluoroethene, both pure *cis*-CHF═CHF and a mixture (~50%) of the *cis*- and the *trans*-form are used as reactants. C_6H_5F (liquid at room temperature) is kept in an ice-cooled vessel, and is led into the reaction chamber as pure vapor or mixed with helium gas.

For laser-induced fluorescence detection, the SrF products are excited by a modified tunable CW dye laser (Spectra Physics Model 375, bandwidth 10 GHz), pumped with the Ar ion laser mentioned above. The probe laser operates with a dye solution of rhodamine 6G to excite the SrF products to the $B\,^2\Sigma$ state (577–587 nm). In the case of $CF_2=CH_2$ also the $A\,^2\Pi_{3/2}-X\,^2\Sigma$ transition (644–653 nm) is used for LIF detection (dye mixture rhodamine 101/rhodamine 6G). The dye laser beam (power in the detection zone ≈35 mW) is mechanically modulated at 120 Hz to allow phase-sensitive amplification of the LIF signal. In the fluorescence detection system the light is spatially and color filtered to suppress scattered laser light and the $Sr(^3P_1)$ fluorescence light. The light is detected as a function of excitation wavelength using a photomultiplier tube (RCA C31034). An etalon, a hollow cathode lamp, and a Burleigh wave meter are used for wavelength calibration.

III. SIMULATION

Table I presents all energy terms, leading to an average available energy for the reaction products, $\langle E_{\mathrm{avl}}\rangle$. The energy distribution function for the internal energy of the molecular reactants E_{int} is convoluted with the distribution function for the collision energy E_{col}, calculated from a Maxwell velocity distribution for the atomic (900 K) and molecular reactants (298 K). The resulting distribution function is then shifted upward by the reaction exothermicity $D_0^o(\mathrm{SrF})-D_0^o(\mathrm{R-F})+E_{\mathrm{Sr}}(^3P_1)$. The uncertainty in $\langle E_{\mathrm{avl}}\rangle$ is dominated by the uncertainties in the bond dissociation energies D_0^o. The last column of Table I gives the spread in the available energy, which is determined by the width of the distribution functions (FWHM).

In the spectrum simulation procedure the rovibronic line positions of the $B\,^2\Sigma-X\,^2\Sigma$ transition are calculated from the spectroscopic constants, as presented in Ref. 1. These are parameters taken from Refs. 9 and 16, slightly adjusted to satisfactorily simulate the high rotational populations. The spectroscopic constants from the $A\,^2\Pi_{3/2}$ state are obtained from Refs. 14, 17, 18. Adjustment of the v-dependent parameters is necessary, because the $A\,^2\Pi$ state has only been studied for low vibrational levels (see Ref. 1).

A Gaussian frequency profile of the broadband excitation laser is taken into account for the calculation of the LIF spectrum from the line positions. Vibrational and rotational population distributions of the SrF products are derived from the experimental LIF spectrum, by varying the energy distri-

TABLE I. Reaction energetics for the reactions Sr+CHF═CH_2, CF_2═CH_2, CHF═CHF and C_6H_5F. All energies are in eV. The last column gives the width of the distribution of E_{avl} (FWHM).

Reactant	$\langle E_{\mathrm{int}}\rangle$	$\langle E_{\mathrm{col}}\rangle$	D_0^o(R–F)	D_0^o(Sr–F)	$E_{\mathrm{Sr}(^3P_1)}$	$\langle E_{\mathrm{avl}}\rangle$	$\Delta(E_{\mathrm{avl}})$
CHF═CH_2	0.052[a]	0.090	5.39±0.04[b]	5.60±0.06[c]	1.798[d]	2.15±0.07	0.16
CF_2═CH_2	0.064[a]	0.099	5.45±0.04[e]	5.60±0.06[c]	1.798[d]	2.11±0.07	0.19
c-CHF═CHF	0.061[a]	0.099	5.19±0.18[f]	5.60±0.06[c]	1.798[d]	2.37±0.19	0.18
t-CHF═CHF	0.065[a]	0.099	5.16±0.19[g]	5.60±0.06[c]	1.798[d]	2.40±0.20	0.18
C_6H_5F	0.105[h]	0.110	5.47±0.04[i]	5.60±0.06[c]	1.798[d]	2.11±0.07	0.19

[a]Calculated from molecular constants given in Ref. 7.
[b]Calculated from $\Delta_f H^{298}(\mathrm{F-CH{=}CH_2})=-1.45\pm0.03$ eV (Refs. 7 and 8), $\Delta_f H^{298}(\mathrm{CH{=}CH_2})=3.10\pm0.03$ eV (Refs. 9 and 10) and $\Delta_f H^{298}(\mathrm{F})=0.82$ eV (Ref. 11).
[c]Recommended value from data in Ref. 11.
[d]Taken from Ref. 12.
[e]Calculated from $\Delta_f H^{298}(\mathrm{CF_2{=}CH_2})=-3.49\pm0.03$ eV (Refs. 7 and 8), $\Delta_f H^{298}(\mathrm{F})$, and $\Delta_f H^{298}(\mathrm{CF{=}CH_2})=1.13\pm0.03$ eV (Ref. 7).
[f]Calculated from $\Delta_f H^{298}(\mathit{cis}\text{-CHF{=}CHF})=-3.08\pm0.10$ eV (Refs. 7 and 13), $\Delta_f H^{298}(\mathrm{F})$, and $\Delta_f H^{298}(\mathit{cis}\text{-CH{=}CHF})=1.28\pm0.15$ eV (Ref. 7).
[g]Calculated from $\Delta_f H^{298}(\mathit{trans}\text{-CHF{=}CHF})=-3.04\pm0.10$ eV (Refs. 11 and 13), $\Delta_f H^{298}(\mathrm{F})=0.82$ eV, and $\Delta_f H^{298}(\mathit{trans}\text{-CH{=}CHF})=1.29\pm0.16$ eV (Ref. 7).
[h]Reference 10.
[i]Calculated from $\Delta_f H^{298}(\mathrm{C_6H_5F})=\Delta1.21$ eV (Ref. 34), $\Delta_f H^{298}(\mathrm{F})$, and $\Delta_f H^{298}(\mathrm{C_6H_5})=3.42\pm0.03$ eV (Ref. 15).

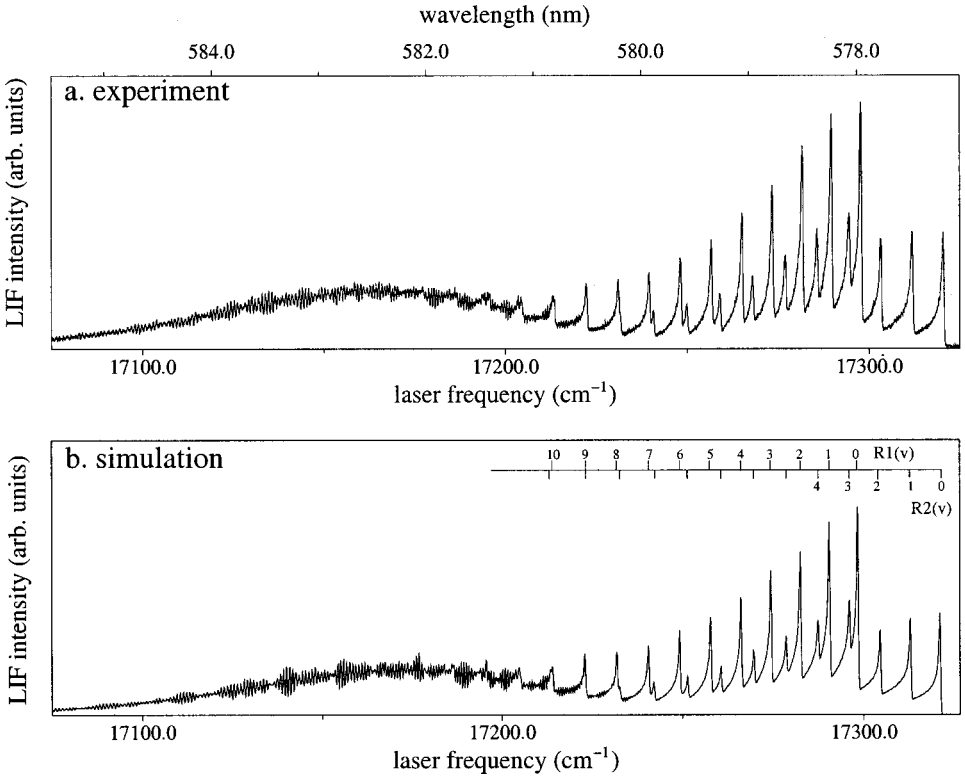

FIG. 2. Experimental (a) and simulated (b) spectra of SrF formed in the reaction of Sr($^3P_1$) with CHF═CH_2. The $B\,^2\Sigma - X\,^2\Sigma$, $\Delta v = 0$ sequence is shown. The simulated spectrum is calculated on the basis of the spectroscopic constants presented in Sec. IV, and the vibrational and rotational state distributions are shown in Fig. 7. A Gaussian frequency profile with a FWHM of 0.4 cm^{-1} is used for the convolution. In the simulated spectrum the R_1 (marks pointing upward) and R_2 bandheads are indicated.

butions used as input in the spectrum simulation program until the experimental spectrum is well reproduced. A correction factor for saturation by optical pumping is used, as was established in previous experiments.[1] Each rovibronic line intensity is multiplied by, $1/(1-0.8q_{v'v''})$, where $q_{v'v''}$ is the Franck–Condon factor of the $v' \leftrightarrow v''$ transition, taken from Refs. 18 and 19 for the $A\,^2\Pi_{3/2}$ and $B\,^2\Sigma$ state, respectively.

IV. RESULTS

In our beam-gas experiments using LIF detection of SrF($X\,^2\Sigma$), we observed no reaction products for the reactions of CHF═CH_2, CF_2═CH_2, CHF═CHF, and C_6H_5F with Sr in its electronic ground state $^1S_0$.

As in our previous studies,[1,2] but in contrast to reactions of nonfluorine containing alkylhalides, i.e., alkylchlorides, bromides, and iodides with electronically excited alkaline earth atoms, which lead to alkaline earth monohalides,[20–24] no experimental evidence was found for chemiluminescent products.

Exciting Sr to the $(5s5p)^3P_1$ state, LIF spectra of SrF($X\,^2\Sigma$) were measured, in most cases using the $B\,^2\Sigma - X\,^2\Sigma$, $\Delta v = 0$ transition. In this transition the R_1 and R_2 branches form bandheads at $N = 150-90$ and $N = 180-120$ for $v = 0-20$, respectively. [N is the quantum number belonging to $\mathbf{N} = \mathbf{J} - \mathbf{S}$, where $\mathbf{J}$ is the total angular momentum (quantum number J), and $\mathbf{S}$ is the electron spin (quantum number $S = \frac{1}{2}$).] The rotational population distribution could be determined accurately from the relative intensity of the bandheads for a certain vibrational level.

Figure 2 presents the experimental (a) and simulated (b) LIF spectrum of SrF formed in the reaction of Sr($^3P_1$) with CHF═CH_2. The spectrum was simulated using a linear surprisal distribution for vibration. The linear surprisal distribution for vibration of the SrF product is given by

$$P^{\lambda_v}(v) \propto (1 - f_v(v))^s e^{-\lambda_v f_v(v)}.$$

The exponent s results from integration over the vibrational and rotational degrees of freedom of the leaving organic radical, the relative translational motion of the reaction products, and the two rotational degrees of freedom of the diatomic product.[25,26] Then $s = N_v + 3$, where N_v is the number of vibrational degrees of freedom of the organic radical. The prior distribution for vibration of the diatomic product is a function of the fractional energy f_v only, and the surprisal is given by the vibrational surprisal parameter λ_v. For SrF formed in the reaction of Sr($^3P_1$) with CH_2═CHF ($N_v = 9$ for the CH_2═CH· product radical), λ_v is found to be -6.9. Note that a negative λ_v denotes higher vibrational excitation of the diatomic product relative to the prior distribution. The rotational state distributions are Gaussian in N peaked at $N = 130$ for $v = 0$ decreasing to $N = 105$ for $v = 10$. The vibrational and rotational state distributions for this and subsequent reactions are given in Fig. 7. From the simulations an average vibrational energy $\langle E_v \rangle = 0.24$ eV and rotational energy $\langle E_r \rangle = 0.48$ eV were deduced (see Table II). For easy reference, the results for saturated fluorohydrocarbons reported previously[2] are also given in Table II.

The average vibrational and rotational energy of the reaction products and the fractional energy disposal as derived from the simulations are presented in Table II. The fractional energy disposed into vibration is given by $\langle f_v \rangle = \langle E_v \rangle / \langle E_{avl} \rangle$, where $\langle E_v \rangle = \Sigma_v E_v P(v) / \Sigma_v P(v)$. Similarly, the fractional rotational energy is defined as $\langle f_r \rangle$

TABLE II. Specific energy disposal into vibration and rotation of the diatomic product. Energies in eV, Δ gives the width of the distribution function (FWHM). The errors in the fractional energies are approximately ±0.01.

Reaction	$\langle E_{avl}\rangle$	$\Delta(\langle E_{avl}\rangle)$	$\langle E_v\rangle$	$\langle f_v\rangle$	$\langle E_r\rangle$	$\langle f_r\rangle$	$\langle E_{t+i}\rangle$	$\langle f_{t+i}\rangle$
Sr+F–CH═CH_2	2.15	0.16	0.28	0.13	0.48	0.22	1.39	0.65
Sr+F–CF═CH_2	2.11	0.19	0.25	0.12	0.35	0.17	1.51	0.71
Sr+*c*-F–CH═CHF	2.37	0.18	0.32	0.14	0.46	0.19	1.59	0.67
Sr+*t*-F–CH═CHF	2.40	0.18	0.22	0.09	0.41	0.17	1.77	0.74
Sr+F–C_6H_5	2.11	0.19	0.19	0.09	0.48	0.23	1.44	0.68
Sr+F–CH_3	2.64	0.13	0.22	0.08	0.87	0.33	1.55	0.59
Sr+F–C_2H_5	2.82	0.18	0.50	0.18	0.61	0.22	1.71	0.61
Sr+F–$CHFCH_3$	2.57	0.20	0.54	0.21	0.48	0.19	1.55	0.60

$=\langle E_r\rangle/\langle E_{avl}\rangle$. The latter two columns present $\langle E_{t+i}\rangle$, the sum of the energy disposed into relative translation of the products and the internal energy of the radical.

Studying the reaction of $Sr(^3P_1)$ with $CF_2=CH_2$, the $B\,^2\Sigma-X\,^2\Sigma$ (Fig. 3) as well as the $A\,^2\Pi_{3/2}-X\,^2\Sigma$ (Fig. 4) transitions were measured. Both spectra could be simulated using the same vibrational and rotational population distributions, viz., a vibrational distribution with $\lambda_v=-5.5$ and Gaussian rotational distributions peaked at $N=105$ for $v=0$ (FWHM, $\Delta N=85$) decreasing to $N=95$ for $v=10$ ($\Delta N=70$). In the $A\,^2\Pi_{3/2}-X\,^2\Sigma$ simulation a contribution of SrF formed in oven reactions had to be taken into account (see Ref. 2). The Q_2/P_{21} branch in this transition forms bandheads at low N ($N=40$), in contrast to the P_2 branch ($N\sim105$) and the R_1, R_2 branches of the $B\,^2\Sigma-X\,^2\Sigma$ transition. Consequently, product molecules with thermal population distributions ($T_v=T_r=900$ K) result in high-intensity bands for $v=0,1$ in the Q_2/P_{21} branch at 15 351.6 and 15 359.6 cm^{-1}, respectively. In Figs. 3 and 4 a contribution of 0.5% thermal product molecules was included. This is hardly visible in the $B\,^2\Sigma-X\,^2\Sigma$ spectrum, since in that transition no bandheads are formed at the low rotational levels that are thermally populated.

Figure 5 presents the experimental (a) and simulated (b) spectra of both pure *cis*-CHF═CHF and a mixture of *cis*- and *trans*-CHF═CHF. Since it is approximately a 1:1 mixture, it is possible to make an estimate of the surprisal distribution of the *trans*-isomer from that of the vibrational distributions for the *cis*-isomer and the mixture, by assuming that the overall reaction cross section is the same for both reactants. The vibrational distribution found for the mixture is very well reproduced by a sum of two surprisal distributions, characterized by two distinct parameters, $\lambda_v(cis)=-7.6$ and $\lambda_v(trans)=-2.0$. Alternatively, the latter distribution can be fitted by a Boltzmann distribution characterized by $T_v=3200$ K. Even if the assumption of equal reaction cross sections is doubtful, it is clear that there is a striking difference in behavior between the isomers in the

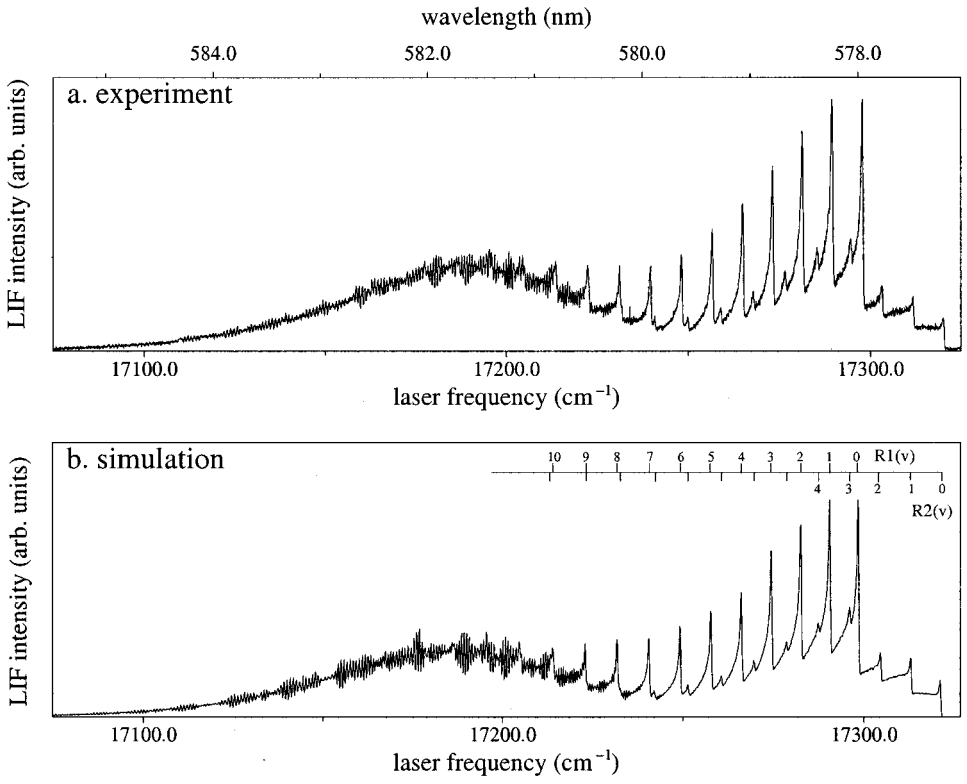

FIG. 3. Experimental (a) and simulated (b) spectra of SrF formed in the reaction of $Sr(^3P_1)$ with $CF_2=CH_2$. The $B\,^2\Sigma-X\,^2\Sigma$, $\Delta v=0$ sequence is shown. The input vibrational and rotational state distributions used in the simulation are shown in Fig. 7. A Gaussian frequency profile with a FWHM of 0.4 cm^{-1} is used for the convolution. The R_1 and R_2 bandheads are indicated.

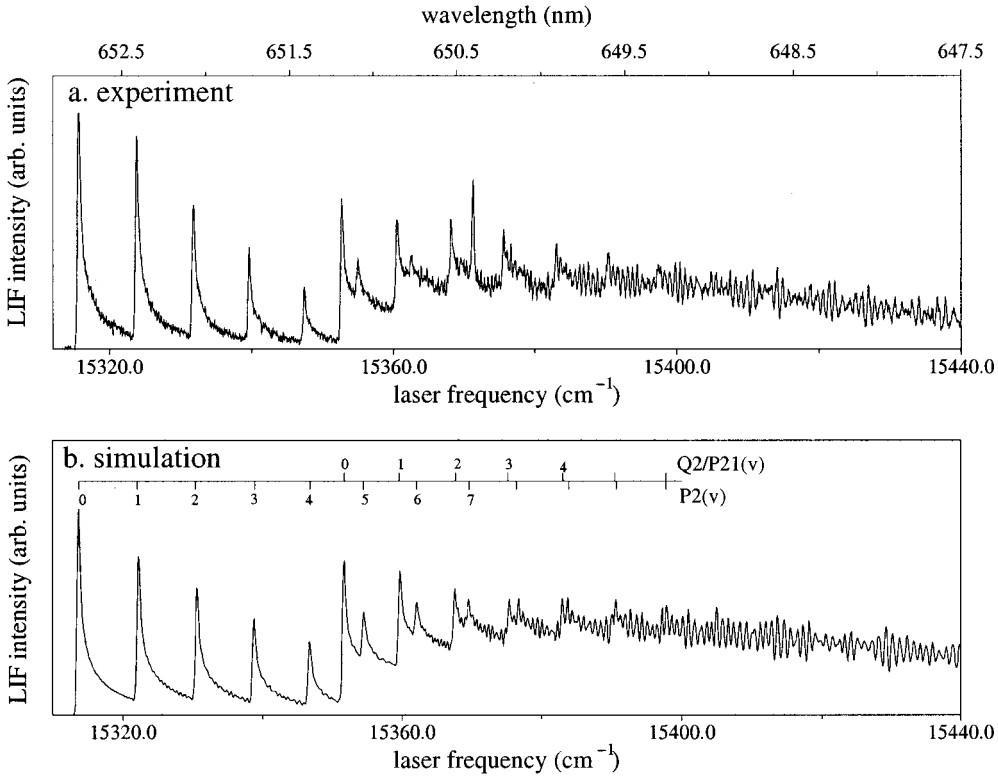

FIG. 4. Experimental (a) and simulated (b) spectra of SrF formed in the reaction of Sr($^3P_1$) with CF_2CH_2. The $A\,^2\Pi_{3/2}-X\,^2\Sigma$, $\Delta v=0$ sequence is shown. For the simulation the spectroscopic constants presented in Sec. IV are used; the intensities are the result of the same vibrational and rotational state distributions used in Fig. 3. A Gaussian frequency profile with a FWHM of 0.4 cm^{-1} is used for the convolution. The Q_2/P_{21} and P_2 bandheads are indicated.

way the energy is disposed in the reaction with Sr($^3P_1$), the *cis*-isomer leading to a larger range of SrF vibrations being excited than the *trans*-isomer. The input vibrational and rotational population distributions used in the simulations are depicted in Fig. 7.

Figure 6 shows the experimental (a) and simulated (b) spectra of SrF($X\,^2\Sigma$) formed in the reaction of electronically excited Sr with C_6H_5F. The vibrational population could be simulated using a Boltzmann distribution characterized by $T_v=2400$ K, and for the rotational population again Gaussian distributions in N are appropriate. Here, a surprisal analysis ($N_v=27$) leads to a less satisfactory fit. The surprisal parameter found is very large and negative: $\lambda_v=-21$.

V. DISCUSSION

Though from our experiment no absolute reaction cross sections can be deduced, we can compare the LIF signal intensities of the SrF($X\,^2\Sigma$) product formed in reactions of Sr($^3P_1$) with the various reactants. The signal intensities in the reactions presented in this study are within the same order of magnitude. Relative to other reactants (CH_3F, C_2H_5F, $C_2H_4F_2$, presented in Ref. 2) the signal intensities at the peak of the v distribution are an order of magnitude stronger. Despite their lower exoergicities the reactions with unsaturated compounds appear to have higher reaction cross sections. In case of the saturated reactants, the vibrational distribution is generally bell-shaped, whereas for the presently studied unsaturated reactants it shows a Boltzmann-type behavior.

A further comparison between fluoroethane and 1,1-difluoroethane, studied in Ref. 2, and the unsaturated reactants, shows that a much lower amount of energy is disposed into vibrational energy of the diatomic product in reactions with unsaturated compounds. Assuming similarly shaped potential surfaces, one would expect that the amount of energy disposed into translation is comparable, since the reduced mass of the reactants and products is about the same for all reactions.

Apparently, the unsaturated organic radicals take up more reaction energy than the saturated radicals (CH_3, C_2H_5, C_2H_4F). Also, the fraction of energy disposed into relative product translation and internal energy of the radical, $\langle f_{t+i}\rangle$, varies with the reactants, contrary to the observations for fluoroethane and for 1,1-difluoroethane, also listed in Table II.[2] The absolute disposal into rotational energy $\langle E_r\rangle$ of the SrF product is observed to be about 27% larger for the reaction with fluoroethane than that with fluoroethene. This result strengthens the suggestion of the presence of distinct reaction mechanisms for these resembling molecular reactants, as discussed below. It is interesting to note that the lower exothermicity of the fluoroethene reaction is not reflected in $\langle f_r\rangle$, which is found to be equal to 0.22 for both reactions (see Table II).

Figure 8 presents two triangle plots, visualizing the internal energy distributions in the SrF($X\,^2\Sigma$) products formed in the reactions of Sr($^3P_1$) with $CHF{=}CH_2$ and C_6H_5F, respectively. As in the previous papers,[1,2] a contour plot is formed by connecting points of fractional energies (f_v, f_r,

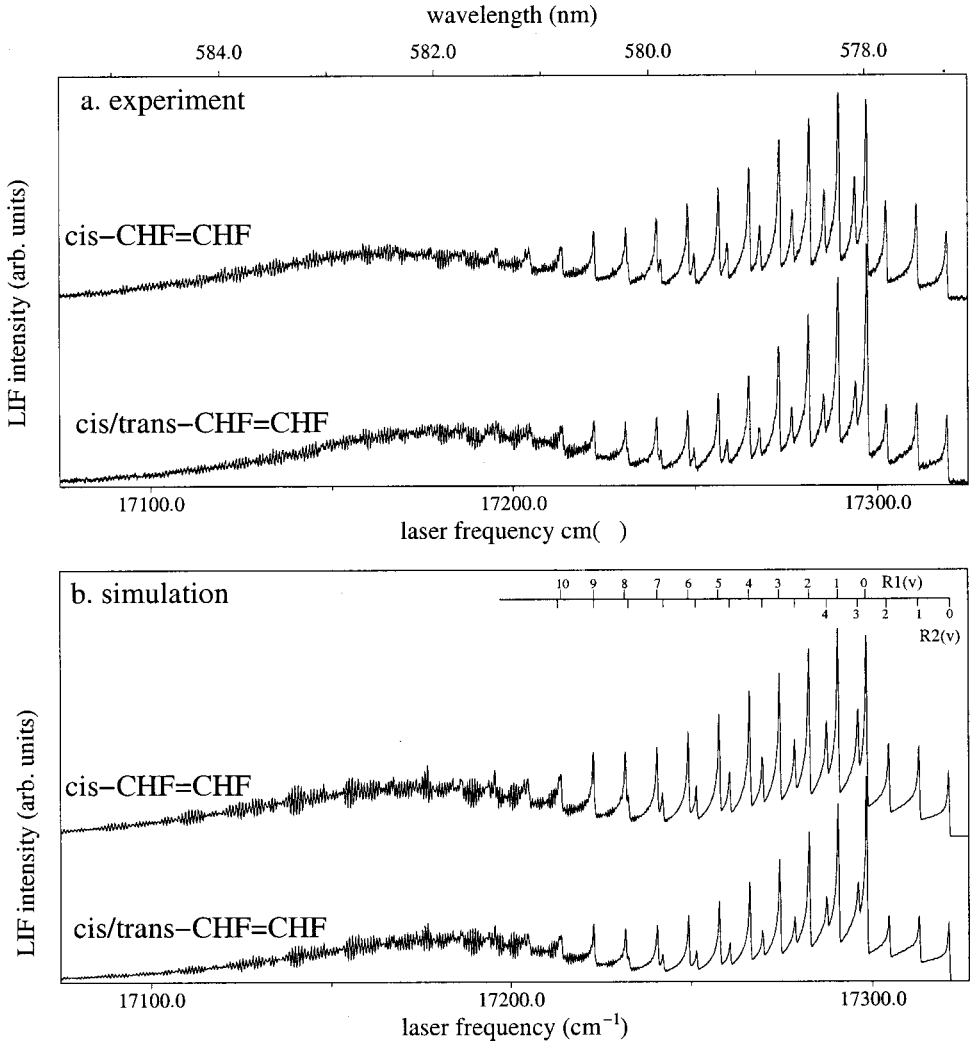

FIG. 5. Experimental (a) and simulated (b) spectra of SrF formed in the reaction of $Sr(^3P_1)$ with *cis*-CHF═CHF and with a mixture of *cis*- and *trans*-CHF═CHF. The $B\,^2\Sigma - X\,^2\Sigma$, $\Delta v = 0$ sequence is shown. For the simulation the spectroscopic constants presented in Sec. IV are used, as well as the vibrational and rotational state distributions shown in Fig. 7. A Gaussian frequency profile with a FWHM of 0.4 cm^{-1} is used for the convolution. The R_1 (marks pointing upward) and R_2 bandheads are indicated.

f_{t+i}) with equal probabilities. The vertices represent situations where all energy is released into one degree of freedom. These plots emphasize the similarity in the product energy distributions for the reactions with fluoroethene and fluorobenzene. It seems as if the total amount of energy disposed into product translation and internal energy of the organic radical, E_{t+i}, does not depend on the size of the unsaturated fluorohydrocarbons. The triangle plots for the product energy distributions in the other reactions presented in this study, viz., $Sr(^3P_1) + CF_2{=}CH_2$, CHF═CHF (*cis*, *trans*), are very similar to the ones shown in Fig. 8, and are therefore not shown. While the triangular plots favor a strong preference for a large f_{t+i}, the obtained vibrational and rotational state distributions of Fig. 7 preclude the presence of severe constraints, limiting the energetically accessible product quantum states, as pointed out by Picconatto, Srivastava, and Valentini,[27] to occur in our study.

The reactions of $Sr(^3P_1)$ with unsaturated fluorohydrocarbons show no strong correlation between vibrational and rotational energy disposed into the diatomic products. Together with the low SrF vibrational energy disposal, this indicates that the reaction dynamics may be dominated by an insertion mechanism. Direct reactions often result in inverted vibrational population distributions in the diatomic product.[28] The presence of a double bond in the molecular reactant possibly supports insertion of the metal in the C–F bond.

In the reaction $Sr(^3P_1) + C_6H_5F$, only 9% of the available energy is disposed into vibrational excitation of the SrF product, despite the large negative value of the surprisal parameter, viz., $\lambda = -22$. This value is not a direct measure of the vibrational energy disposed into the diatomic product. It tells us that relatively much energy is disposed as vibrational energy of the diatomic product, compared to the prior distribution that takes all 27 vibrational degrees of freedom of the leaving organic radical into account as possible reservoirs for energy disposal. The energy disposal in the reaction with C_6H_5F is very similar to that in the reactions with the fluoroethenes, suggesting that the number of internal degrees of freedom coupled to that of the reaction coordinate does not increase going from fluoroethene to fluorobenzene. Compared to previously studied reactions, the fraction of available energy disposed into SrF vibration is small. It is also small compared to the results of Han, He, and Lou of the reactions $Ba + C_6H_5X$ (X=I, Br, Cl). They report fractional vibrational energies of 22%, 29%, and 40% for BaI, BaBr, and BaCl, respectively.[4]

Previously, Loesch and Möller[29–31] rationalized their re-

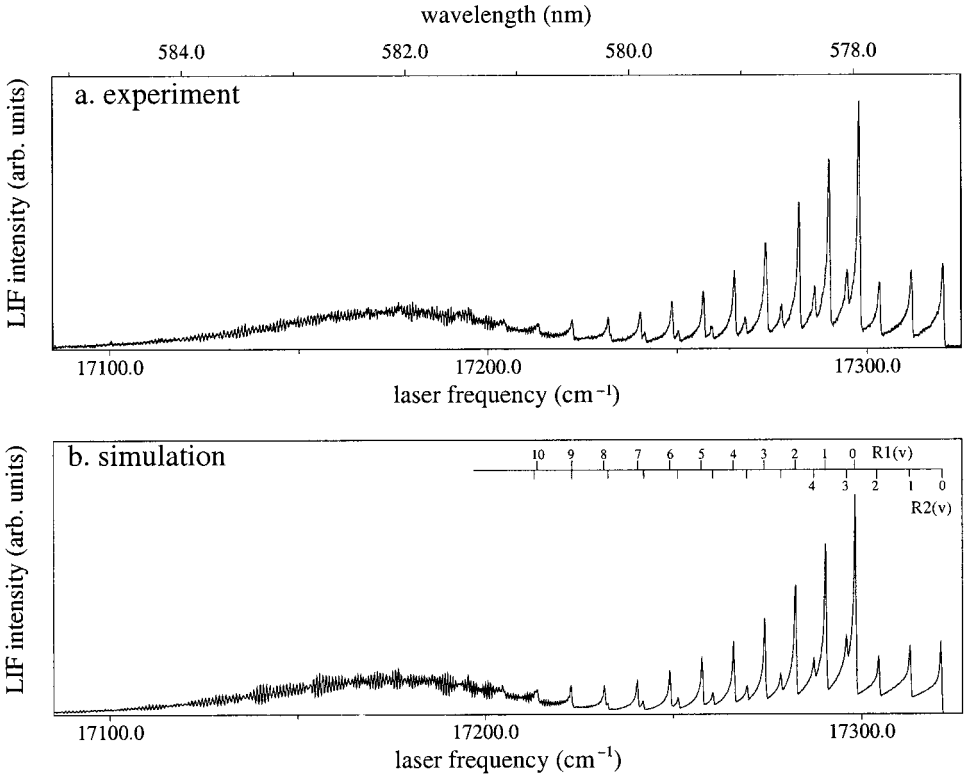

FIG. 6. Experimental (a) and simulated (b) spectra of SrF formed in the reaction of $Sr(^3P_1)$ with C_6H_5F. The $B\,^2\Sigma - X\,^2\Sigma$, $\Delta v = 0$ sequence is shown. The input vibrational and rotational state distributions used in the simulation are shown in Fig. 7. A Gaussian frequency profile with a FWHM of $0.4\,cm^{-1}$ is used for the convolution. The R_1 and R_2 bandheads are indicated.

sults of scattering experiments on K with different iodides, in terms of MO theory. Following similar arguments, the different behavior of the vibrational population of SrF for reactions of saturated versus unsaturated reactant molecules could be rationalized as follows in terms of simple MO theory,[32] and assuming a harpoon mechanism. As a first step in the reaction, the electron is supposed to jump from Sr to the LUMO of the reactant molecule. Actually, the orbital is deformed by the approach of the Sr atom, but we assume that it still has the characteristics of the original LUMO. For reactions with alkylfluorides, the electron will jump to the C–F σ^* orbital, which is strongly repulsive, and the molecule will undergo very fast dissociation into R· and F^- (compare Refs. 4, 5, 29–31). For reactions with fluorine substituted ethenes and for fluorobenzene, the electron is also supposed to make a transfer to the LUMO, which in this case is a π^* orbital. The orbital has a slightly nonbonding or antibonding character in the C–F bond, so that this bond is expected to become slightly weaker (cf. Ref. 33). Dissociation from this state would result in a negative molecular ion and a F atom, so another transfer of the electron to a C–F σ^* orbital is necessary, corresponding to a strongly repulsive state, to allow for the release of F^-. As a function of the C–F bond length, the π^* state and the σ^* state correspond with a nondissociative and a strongly repulsive potential energy curve, respectively. If the C–F bond is weakened sufficiently by the electron in the π^* state, the bond length will increase to the point where the potential curves cross, so that a smooth transition of the electron to the σ^* state may occur. Consequently, compared to the reactions with alkylfluorides, the reaction path will be extended. This will enhance the probability of scrambling of the energy carried by the reaction coordinate by its prolonged coupling to other vibrational modes. This could explain why the vibrational distribution for the reactions of Sr with the unsaturated hydrocarbons decreases steeply with v.

However appealing such a picture may be, it does not explain why the vibrational energy distributions of SrF resulting from the reactions with *cis*- and *trans*-difluoroethene (the distribution for the latter reactant being derived as described in Sec. IV) are clearly different, the vibrational surprisal parameters being -7.6 and -2.0 for *cis*- and *trans*-difluoroethene, respectively. For an explanation of this result, a much more demanding quantum mechanical approach will be required.

Comparing the experimental LIF spectra obtained in the present study (Figs. 2, 3, 5, and 6), subtle but significant differences are observed. In Fig. 3, for example, the intensity of the R_2 bandheads is much lower than in the other figures, indicating lower rotational excitation in the $SrF(X\,^2\Sigma)$ reaction product in the reaction with $CF_2{=}CH_2$. Indeed, this is deduced from the spectra by simulation, as can be seen both in the rotational population distributions (Fig. 7) and Table II.

Similar to our observations in a previous paper concerning mono- and 1,1-difluoroethane,[2] 1,1-difluoroethene shows lower rotational excitation in the SrF products and narrower population distributions than monofluoroethene. This suggests that two geminal fluorine atoms reduce the range of angles at which the SrF molecule can leave the reaction center, resulting in narrow population distributions. On the other hand, the rotational distributions for the reaction with C_6H_5F show population distributions of comparable widths, which makes the above suggestion dubious.

In summary, the series of experiments in this and previous studies[1,2] and on the reactions of electronically excited

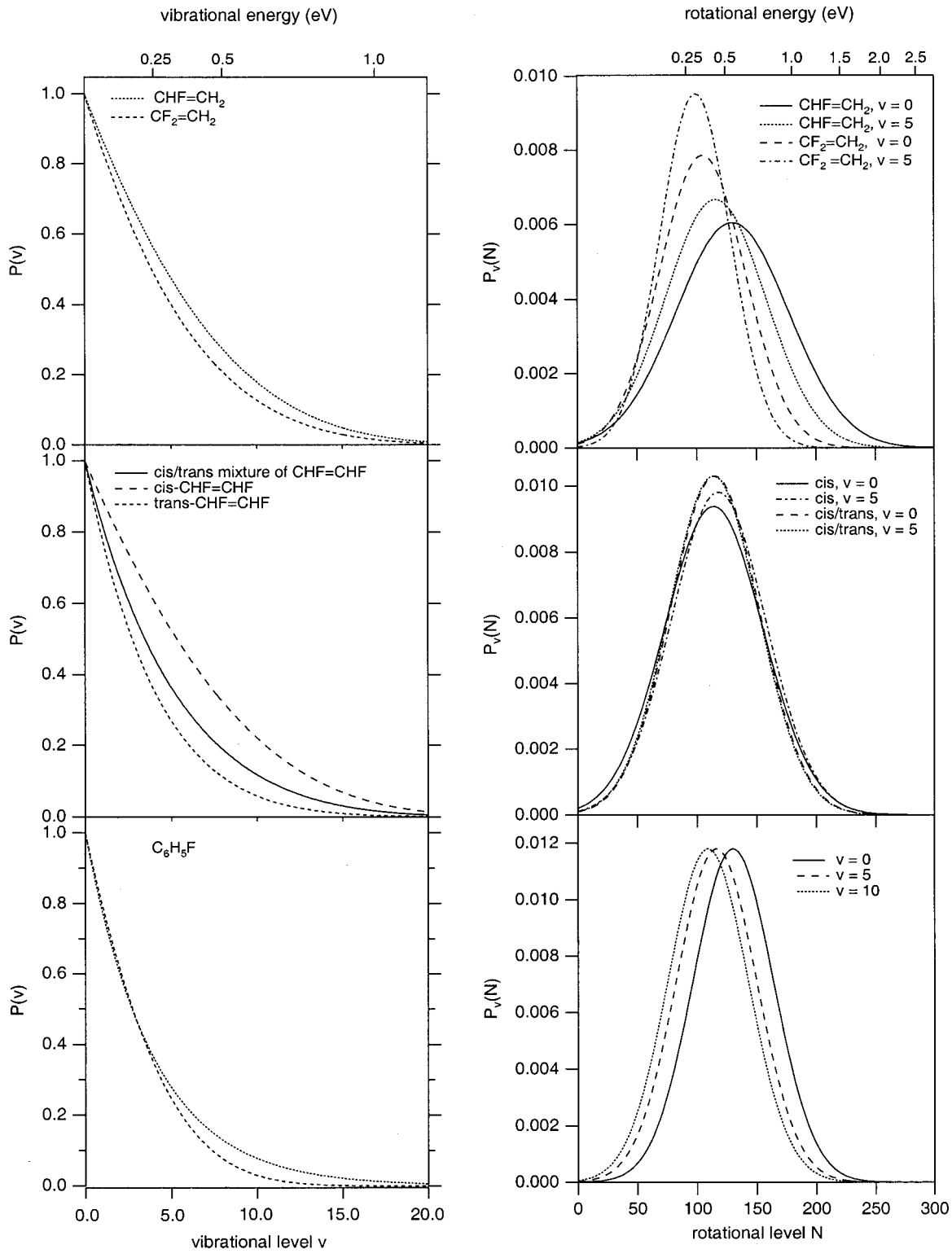

FIG. 7. Input vibrational and rotational population distributions used in the simulated LIF spectra of SrF formed in the reaction of $Sr(^3P_1)$ with $CHF{=}CH_2$, $CF_2{=}CH_2$ (top), *cis*- and *trans*-$CHF{=}CHF$ (center), and C_6H_5F (bottom). The vibrational state distributions for the $CHF{=}CH_2$, $CF_2{=}CH_2$, *cis*-$CHF{=}CHF$ reactions are surprisal distributions defined by $\lambda_v=-6.9$, $\lambda_v=-5.5$, and $\lambda_v=-7.6$, respectively. The vibrational population for the 1:1 mixture of *cis* and *trans*-$CHF{=}CHF$ can be taken as a linear superposition $[(1-f_v)^{12}\exp(7.6f_v)+(1-f_v)^{12}\exp(2.0f_v)/2.74]$ of the surprisal distribution for the *cis*-isomer $[(1-f_v)^{12}\exp(7.6f_v)]$ and a hypothetical surprisal distribution for the *trans*-isomer $[(1-f_v)^{12}\exp(2.0f_v)]$, under the assumption that the reaction cross sections of the *cis*- and *trans*-isomers are equal. The vibrational distribution for the reaction with C_6H_5F can also be represented by a surprisal analysis, with $\lambda_v=-22$, i.e., $(1-f_v)^{30}\exp(22\,f_v)$ (dashed line). The bandhead intensities in the LIF spectrum of SrF from the $Sr^*+C_6H_5F$ reaction are better for $v>7$ if a Boltzmann distribution is used, characterized by $T_v=2400$ K (dotted line). The rotational state distributions are Gaussian distributions in N peaked at $N=130$ for $v=0$ in case of $CHF{=}CH_2$ and C_6H_5F, $N=120$ for $v=0$ in case of $CHF{=}CHF$, and $N=105$ for $v=0$ in case of $CF_2{=}CH_2$. The distributions differ in width, and shift to lower rotational levels for larger v.

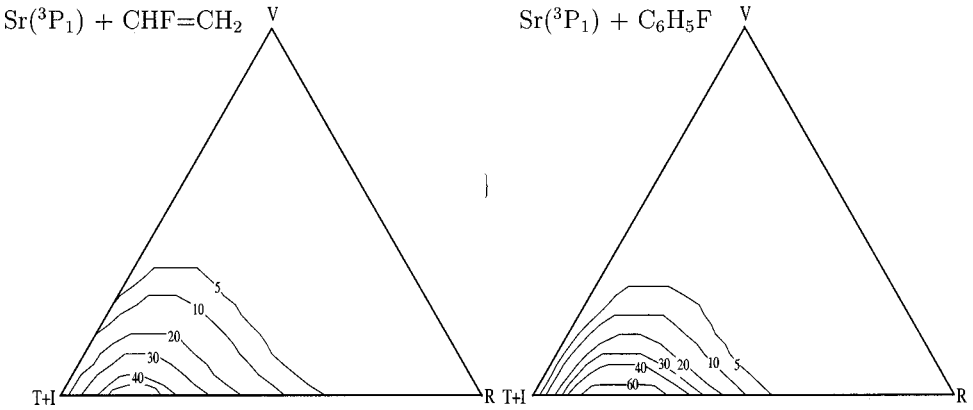

FIG. 8. Triangular plots of energy disposal in the $Sr(^3P_1)+CHF{=}CH_2$ and C_6H_5F reactions. The experimental results are displayed as contours of relative populations in a triangular coordinate system (see the text). V=vibration, R=rotation, $T+I$ =relative translation+internal energy organic radical.

Sr with fluor containing molecules illustrates the large influence of the organic radical in the formation of the $SrF(X\,^2\Sigma)$ product. Generally, reactions with HF and saturated fluorohydrocarbons result in inverted vibrational energy distributions, whereas in the reactions presented in the present paper the energy is distributed almost statistically. The energy disposal in the reaction with C_6H_5F is very similar to that in the reactions with the fluoroethenes, despite the difference in the size of the reactants.

Subtle but significant differences are observed between reactions with various configurations of $C_2H_2F_2$. However, the energy disposal mechanism is complex, and a complete interpretation of our experimental observations requires more experimental (e.g., measurements of the recoil distribution among the products) and theoretical work.

ACKNOWLEDGMENTS

This research has been financially supported by the Councils for Chemical and Physical Sciences of the Netherlands Organization for Scientific Research (CW- and FOM-NWO). The authors gratefully acknowledge clarifying comments by Professor R. D. Levine, in particular, on the surprisal analysis, and the elucidating discussions with Dr. F. M. Bickelhaupt on the validity of the MO picture. The authors also thank Dr. M. C. van Hemert and Dr. C. A. Taatjes for enlightening contributions.

[1] J. M. Teule, J. Mes, J. Bulthuis, M. H. M. Janssen, and S. Stolte, J. Phys. Chem. A **102**, 9482 (1998).
[2] J. M. Teule, M. H. M. Janssen, J. Bulthuis, and S. Stolte, J. Chem. Phys. **110**, 10792 (1999).
[3] F. Keijzer, J. M. Teule, J. Bulthuis, G. J. de Graaff, M. H. Hilgeman, M. H. M. Janssen, E. H. van Kleef, J. J. van Leuken, and S. Stolte, Chem. Phys. **207**, 261 (1996).
[4] K. Han, G. He, and N. Lou, Chem. Phys. Lett. **203**, 509 (1993).
[5] K. Han, G. He, and N. Lou, Chem. Phys. Lett. **193**, 165 (1992).
[6] D. M. Brenner, G. P. Smith, and R. N. Zare, J. Am. Chem. Soc. **98**, 6707 (1976).
[7] M. R. Zachariah, P. R. Westmoreland, D. R. Burgess, Jr., W. Tsang, and C. F. Melius, J. Phys. Chem. **100**, 8737 (1996).
[8] L. Gurvich, I. V. Veyts, and C. B. Alcock, in *Thermodynamic Properties of Individual Substances* (Hemisphere, New York, 1991).
[9] T. C. Steimle, P. J. Domaille, and D. O. Harris, J. Mol. Spectrosc. **68**, 134 (1977).
[10] *Handbook of Chemistry and Physics*, 77th ed. (CRC, Boca Raton, 1996).
[11] M. W. Chase, C. A. Davies, J. R. Downey, D. J. Frurip, R. A. McDonald, and A. N. Syverud, J. Phys. Chem. Ref. Data Suppl. **14**, 1 (1985).
[12] A. A. Radzig and B. H. Smirnov, *Reference Data on Atoms, Molecules and Ions* (Springer-Verlag, Berlin, 1980).
[13] H. W. Jochims, W. Lohr, and H. Baumgärtel, Nouv. J. Chim. **3**, 109 (1979).
[14] T. C. Steimle, P. J. Domaille, and D. O. Harris, J. Mol. Spectrosc. **73**, 441 (1978).
[15] J. Berkowitz, G. B. Ellison, and D. Gutman, J. Phys. Chem. **98**, 2744 (1994).
[16] W. E. Ernst and J. O. Schröder, Chem. Phys. **78**, 363 (1983).
[17] T. C. Steimle, D. A. Fletcher, and C. T. Scurlock, J. Mol. Spectrosc. **158**, 487 (1993).
[18] F. Stienkemeier, Ph.D. thesis, University of Bielefeld, 1993.
[19] W. Kinner, Ph.D. thesis, University of Bielefeld, 1990.
[20] J. M. Orea, A. Laplaza, C. A. Rinaldy, G. Tardajos, and A. Gónzalez Ureña, Chem. Phys. **222**, 337 (1997).
[21] C. A. Rinaldy, C. M. Santiveri, G. Tardajos, and A. E. Gónzalez Ureña, Chem. Phys. Lett. **274**, 29 (1997).
[22] M. Wang, K. Han, J. Zhan, V. Wu, G. He, and N. Lou, Chem. Phys. Lett. **278**, 307 (1997).
[23] M. Wang, K. Han, J. Zhan, V. Wu, G. He, and N. Lou, Chem. Phys. Lett. **317**, 220 (2000).
[24] B. Pranszke, P. Kierzkowski, and A. Kowalski, Chem. Phys. Lett. **309**, 183 (1999).
[25] E. Zamir and R. D. Levine, Chem. Phys. **52**, 253 (1980).
[26] F. Keijzer, Ph.D. thesis, Katholieke Universiteit Nijmegen, 1992.
[27] C. A. Picconatto, A. Srivastava, and J. J. Valentini, J. Chem. Phys. **114**, 1663 (2001).
[28] R. Zhang, D. J. Rakestraw, K. G. McKendrick, and R. N. Zare, J. Chem. Phys. **89**, 6283 (1988).
[29] H. J. Loesch and J. Möller, J. Phys. Chem. A **101**, 7534 (1997).
[30] H. J. Loesch and J. Möller, J. Phys. Chem. **97**, 2158 (1993).
[31] H. J. Loesch and J. Möller, J. Chem. Phys. **97**, 9016 (1992).
[32] T. A. Albright, J. K. Burdett, and M.-H. Wangbo, *Orbital Interactions in Chemistry* (Wiley-Interscience, New York, 1985).
[33] D. D. Clarke and C. A. Coulson, J. Chem. Soc. A **1969**, 169.
[34] R. C. Reid, J. M. Prausnitz, and B. E. Poling, *The Properties of Gases and Liquids*, 4th ed. (McGraw-Hill, Singapore, 1988).